A Cross-Coupled Type AC-DC Converter for Remote Power Feeding to a RFID Tag

KEI EGUCHI
Shizuoka University
Department of Technology Education
836, Ohya, Shizuoka, 422-8529
JAPAN
ekeguch@ipc.shizuoka.ac.jp

TAKAHIRO INOUE
Kumamoto University
Department of Electrical and Computer Engineering
2-40-1, Kurokami, Kumamoto, 860-8555
JAPAN
pt-inoue@cs.kumamoto-u.ac.jp

ICHIROU OOTA
Kumamoto National College of Technology
Department of Information and Communication
2659-2, Suya, Koushi, Kumamoto, 861-1102
JAPAN
oota-i@tc.knct.ac.jp

HONGBING ZHU
Hiroshima Kokusai Gakuin University
Department of Computer Science
6-20-1, Nakano, Akiku, Hiroshima, 739-0321
JAPAN
kohe@wuchang.cs.hkg.ac.jp

FUMIO UENO
Sojo University
Department of Software Science
4-22-1, Ikeda, Kumamoto, 860-0082
JAPAN
ueno-f@cis.sojo-u.ac.jp

Abstract: In this paper, a cross-coupled type AC-DC converter for RFID tags is proposed. The converter consists of 2 charge-pump type AC-DC converters with opposite polarities. In conventional converters, the threshold voltage of a diode switch causes the decrease in power efficiency. By using cross-coupled connection of CMOS switches, the proposed converter can alleviate the influence of the threshold voltage. Hence, it can achieve an AC-DC conversion with high efficiency. Furthermore, the circuit size of the proposed converter is almost the same as that of the conventional circuit. Through SPICE simulations, the following characteristics are obtained: 1. the power efficiency is more than 88 % and 2. the electric power is about 5mW when an output load is 500 Ω. Concerning the power efficiency and the ripple voltage, theoretical design formulas are derived. Furthermore, the validity of the circuit design is confirmed by experiments.

Key–Words: AC-DC Converters, Switched-Capacitor Circuits, Charge-Pump Circuits, Power Converters, RFID Tags, RF Electromagnetic Induction

1 Introduction

RFID (Radio Frequency IDentification) systems manage information with tags which embedded non-contact radio chips. Recently, RFID tags [1-13] attract much attention as a basic technology of IT (Information Technology). Concretely, they are used in the fields of traffic control [6], security systems [9], etc. [1-13]. In our laboratory, a RFID tag is being developed to measure biomedical signals of transgenic mice [10-13]. In order to supply electric power to the RFID tag implanted into the transgenic mice, remote power feeding is used in the system. The RFID tag is classified into an active-type and a passive-type. However, in the active-type, an external battery is required in order to operate a tag. Therefore, we employ the passive-type RFID tags, because the size of active-type RFID tags is large and heavy.

In the passive-type RFID tags, the remote power feeding is achieved by using RF electro-magnetic induction. Therefore, to convert AC voltages provided by power receiving coils, AC-DC converters [10-17] are necessary in the tags. For example, step-up type AC-DC converters are employed in the RFID tags proposed in [10-13]. These converters consist of diode switches and capacitors. In the design of the AC-DC

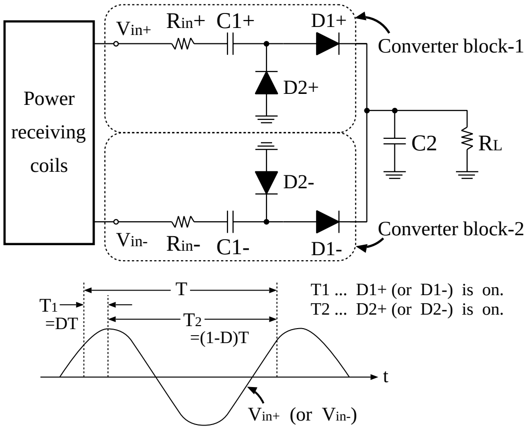

Fig.1 Conventional AC-DC converter.

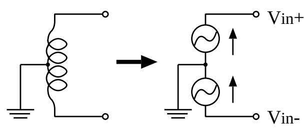

Fig.2 Power receiving coils.

converters for RFID tags, to suppress adverse effects caused by heat, the converters which can realize high power efficiency as well as small chip area are desirable. However, in the conventional converters [11-13], threshold voltage drop caused by diode-switches decreases the power efficiency.

In this paper, a cross-coupled type AC-DC converter for RFID tags is proposed. The converter consists of 2 charge-pump type [18-22] AC-DC converters with opposite polarities. Instead of the diode-switches, the proposed converter employs CMOS switches which are controlled by using cross-coupled connection. Hence, it can achieve an AC-DC conversion with high efficiency, because the cross-coupled connection of CMOS switches alleviates the threshold voltage drop. Furthermore, the circuit size of the proposed converter is almost the same as that of the conventional circuit.

The circuit design and characteristics of the converter are analyzed through theoretical analyses and simulations, and the experimental circuit is fabricated with commercially available transistors.

2 Circuit Structure

2.1 Conventional Converter

Figure 1 shows a charge-pump type AC-DC converter proposed in [11-13]. In RFID tag systems, remote power feeding systems using RF electromagnetic induction are used. In Fig.1, a pair of power receiving coils is modeled by a pair of AC voltage sources with opposite polarities. Figure 2 shows a model the power receiving coils. The conventional converter of Fig.1 consists of 2 charge-pump type AC-DC converters with opposite polarities. The converter shown in Fig.1 can supply a stepped-up DC voltage. After the AC-DC conversion, the output DC voltage is regulated by a series regulator.

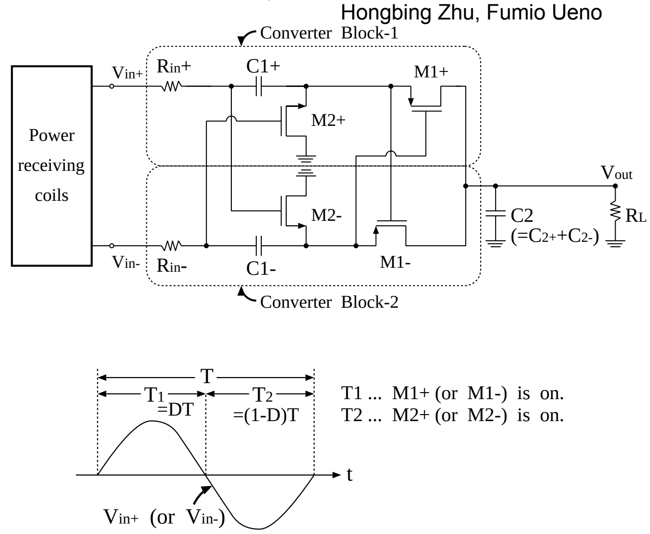

Fig.3 Proposed AC-DC converter.

For easy understanding of the circuit operation, let us consider the converter block-1. When the input voltage V_{in+} is in $State - T2$ [1] (see in Fig.1), the diode D_{2+} is turned on. Then the voltage of C_{1+} becomes about $V_m - V_{th}$, where V_m and V_{th} denote the amplitude voltage of AC input and the threshold voltage of the diode, respectively. Next, when the input voltage V_{in+} is in $State - T1$ (see in Fig.1), the diode D_{1+} is turned on. Then the output voltage of the converter becomes about $2(V_m - V_{th})$. Hence, the threshold voltage drop caused by diodes affects the power efficiency of the conventional converter. In this paper, we solve this problem by using cross-coupled connection of CMOS switches.

2.2 Proposed Converter

Figure 3 shows the proposed AC-DC converter. The converter is designed to receive power by electromagnetic induction in the dozens MHz range. In Fig.3, MOS transistors are used instead of the diodes in Fig.1. As Figs.1 and 3 show, the circuit size of the proposed converter is almost the same [2] as that of the

[1] In Fig.1, D denotes a duty factor.

[2] The conventional converter of Fig.1 consists of 4 diode-switches and 3 capacitors. On the other hand, the proposed converter of Fig.3 can be constructed with 4 MOS switches and 3

conventional circuit. The operation of the converter block-1 is as follows.

When the input voltage V_{in+} is in $State-T2$ (see in Fig.3), the transistor M_{2+} is turned on, because the gate terminal of M_{2+} is connected to another input terminal with opposite polarity, V_{in-}. Therefore, the voltage of C_{1+} becomes V_m. At the same time, the transistor M_{1+} is turned off since the gate terminal of M_{1+} is connected to the right terminal of C_{1-} [3].

Next, when the input voltage V_{in+} is in $State-T1$ (see in Fig.3), the transistor M_{2+} is turned off. At the same time, the transistor M_{1+} is turned on, because the gate terminal of M_{1+} is grounded via M_{2-}. Hence, the output voltage of the converter becomes about $2V_m$. By iterating these operations, the proposed converter supplies a stepped-up DC voltage.

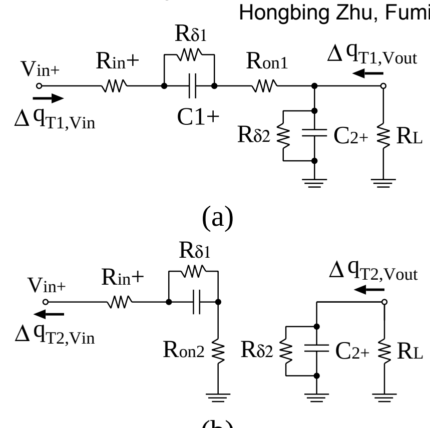

Fig.4 Instantaneous equivalent circuits of converter block-1. (a) $State-T1$. (b) $State-T2$.

3 Theoretical Analysis

3.1 Equivalent Circuit and Power Efficiency

The equivalent circuit and the power efficiency of the proposed converter are analyzed theoretically. To simplify the theoretical analyses, we assume that the time constant R_LC_{2+} and R_LC_{2-} are quite larger than T and parasitic elements are not effective.

Firstly, the equivalent circuit of the converter block-1 is analyzed. The instantaneous equivalent circuits of the converter block can be expressed by the circuits shown in Fig.4. In Fig.4, $R_{\delta k}$ $(k=1,2)$ denotes a resistor to model a dielectric loss.

In the steady state, the differential values of the electric charges in C_{1+} and C_{2+} satisfy

$$\Delta q_{T1}^k + \Delta q_{T2}^k = 0 \qquad (k=1,2), \qquad (1)$$

where Δq_{T1}^k and Δq_{T2}^k denote the electric charges when $T1$ and $T2$, respectively. The intervals of $State-T1$ and $State-T2$, $T1$ and $T2$, satisfy the following conditions:

$$\begin{aligned} & T = T1 + T2, \\ & T1 = DT, \\ \text{and} \qquad & T2 = (1-D)T, \end{aligned} \qquad (2)$$

where T is a period of the input voltage and D denotes a duty factor (see in Fig.3).

In the case of $State-T1$, the currents which flow C_{k+} and $R_{\delta k}$ are given by

$$\Delta q_{T1}^k / T_1 \quad \text{and} \quad (q_{T1}^k/T_1)\tan\delta_k,$$

respectively, where δ_k denotes a dielectric loss angle. Thus the differential values of the electric charges in the input and the output terminals, $\Delta q_{T1,V_{in}}$ and $\Delta q_{T1,V_{out}}$, are given by

$$\begin{aligned} \Delta q_{T1,V_{in}} &= \Delta q_{T1}^1(1+\tan\delta_1) \\ \text{and} \qquad \Delta q_{T1,V_{out}} &= \Delta q_{T1}^2(1+\tan\delta_2) \\ &\quad -\Delta q_{T1}^1(1+\tan\delta_1), \end{aligned} \qquad (3)$$

respectively. On the other hand, in the case of $State-T2$, the currents which flow C_{k+} and $R_{\delta k}$ are given by

$$\Delta q_{T2}^k / T_2 \quad \text{and} \quad (q_{T2}^k/T_2)\tan\delta_k,$$

respectively. Thus $\Delta q_{T2,V_{in}}$ and $\Delta q_{T2,V_{out}}$, are given by

$$\begin{aligned} \Delta q_{T2,V_{in}} &= \Delta q_{T2}^1(1+\tan\delta_1) \\ \text{and} \qquad \Delta q_{T2,V_{out}} &= \Delta q_{T2}^2(1+\tan\delta_2), \end{aligned} \qquad (4)$$

respectively. Here, the electric charges in the input and the output, $\Delta q_{V_{in}}$ and $\Delta q_{V_{out}}$, are given by

$$\begin{aligned} \Delta q_{V_{in}} &= \Delta q_{T1,V_{in}} + (-\Delta q_{T2,V_{in}}) \\ \text{and} \qquad \Delta q_{V_{out}} &= \Delta q_{T1,V_{out}} + \Delta q_{T2,V_{out}}, \end{aligned} \qquad (5)$$

respectively. By substituting Eqs.(1), (3), and (4) into Eq.(5), the following equations are derived:

$$\begin{aligned} \Delta q_{V_{in}} &= 2\Delta q_{T1}^1(1+\tan\delta_1), \\ \Delta q_{V_{out}} &= -\Delta q_{T1}^1(1+\tan\delta_1), \\ \Delta q_{V_{in}} &= -2\Delta q_{V_{out}}, \\ \text{and} \qquad \overline{I_{in}} &= -2\overline{I_{out}}, \end{aligned} \qquad (6)$$

where $\overline{I_{in}}$ and $\overline{I_{out}}$ denote an averaged input current and an averaged output current, respectively.

capacitors.

[3]In this timing, the node voltage of the right terminal of C_{1-} is about $2V_m$.

In Fig.4, the energy consumed by resistors in 1-period, W_{SC}, can be expressed by

$$W_{SC} = W_{T1} + W_{T2}, \tag{7}$$

where

$$W_{T1} = \frac{(R_{in} + R_{on1}) \cdot \{\Delta q_{T1}^{1}(1 + \tan\delta_1)\}^2}{T1} + \frac{R_{\delta 1} \cdot (\Delta q_{T1}^{1} \tan\delta_1)^2}{T1} + \frac{R_{\delta 2} \cdot (\Delta q_{T1}^{2} \tan\delta_2)^2}{T1}$$

and

$$W_{T2} = \frac{(R_{in} + R_{on2}) \cdot \{\Delta q_{T2}^{1}(1 + \tan\delta_1)\}^2}{T2} + \frac{R_{\delta 2} \cdot (\Delta q_{T2}^{2} \tan\delta_2)^2}{T2}.$$

In Fig.4 (a) and (b), the following equations can be obtained by Kirchhoff's law:

$$\begin{aligned} \overline{V_{in}} \cdot T1 &= R_{\delta_2} \Delta q_{T1}^{2} \tan\delta_2 - R_{\delta_1} \Delta q_{T1}^{1} \tan\delta_1 \\ &- (R_{in} + R_{on1})(1 + \tan\delta_1)\Delta q_{T1}^{1} \end{aligned}$$

and

$$\begin{aligned} -\overline{V_{in}} \cdot T2 &= R_{\delta_1} \Delta q_{T2}^{1} \tan\delta_1 \\ &+ (R_{in} + R_{on2})(1 + \tan\delta_1)\Delta q_{T2}^{1}. \end{aligned} \tag{8}$$

By substituting Eq.(2) into (8), the following equation can be derived:

$$\begin{aligned} &\Delta q_{T1}^{2} \tan\delta_2 = \\ &\quad \Delta q_{T1}^{1} \cdot \frac{D}{R_{\delta_2}} \{(R_{\delta_1} \tan\delta_1)(\frac{1}{D} + \frac{1}{1-D}) \\ &\quad + (1 + \tan\delta_1)(\frac{R_{in} + R_{on1}}{D} + \frac{R_{in} + R_{on2}}{1-D})\}. \end{aligned} \tag{9}$$

When the proposed circuit satisfies the following conditions:

$$\begin{aligned} & D = 1/2, \\ & R_{on} \equiv R_{on1} = R_{on2}, \\ & R_{\delta} \equiv R_{\delta 1} = R_{\delta 2}, \\ \text{and} \quad & \tan\delta \equiv \tan\delta_1 = \tan\delta_2, \end{aligned} \tag{10}$$

Eq.(9) can be rewritten as

$$\begin{aligned} \Delta q_{T1}^{2} \tan\delta &= -\Delta q_{V_{out}} \cdot \frac{2}{R_{\delta}(1 + \tan\delta)} \\ &\cdot \{R_{in} + R_{on} + (R_{in} + R_{on} + R_{\delta}) \tan\delta\}. \end{aligned} \tag{11}$$

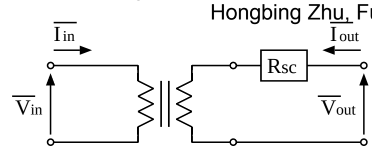

Fig.5 Equivalent circuit of step-up SC converter.

Under the conditions of Eq.(10), we derive the following equations by substituting Eqs.(1), (6) and (11) into Eq.(7):

$$\begin{aligned} W_{T1} &= 2(R_{in} + R_{on}) \frac{(\Delta q_{V_{out}})^2}{T} \\ &+ 2R_{\delta} (\frac{\tan\delta}{1 + \tan\delta})^2 \frac{(\Delta q_{V_{out}})^2}{T} \\ &+ 2R_{\delta} [\frac{2\{R_{in} + R_{on} + (R_{in} + R_{on} + R_{\delta}) \tan\delta\}}{R_{\delta}(1 + \tan\delta)}]^2 \\ &\cdot \frac{(\Delta q_{V_{out}})^2}{T} \end{aligned}$$

and

$$\begin{aligned} W_{T2} &= 2(R_{in} + R_{on}) \frac{(\Delta q_{V_{out}})^2}{T} \\ &+ 2R_{\delta} [\frac{2\{R_{in} + R_{on} + (R_{in} + R_{on} + R_{\delta}) \tan\delta\}}{R_{\delta}(1 + \tan\delta)}]^2 \\ &\cdot \frac{(\Delta q_{V_{out}})^2}{T}. \end{aligned} \tag{12}$$

Here, it is known that a general equivalent circuit of SC power converters can be expressed by the circuit of Fig.5 [23-25], where $\overline{V_{in}}$ denotes an averaged voltage of $|V_{in+}|$ (or $|V_{in-}|$) and $\overline{V_{out}}$ is an averaged voltage of V_{out}. The consumed energy W_{SC} in Fig.5 is defined by

$$\begin{aligned} W_{SC} &= W_{T1} + W_{T2} \\ &\equiv (\frac{\Delta q_{V_{out}}}{T})^2 \cdot R_{SC} \cdot T. \end{aligned} \tag{13}$$

From Eqs.(12) and (13), the resistance R_{SC} in Fig.5 is expressed by

$$\begin{aligned} R_{SC} &= 4(R_{in} + R_{on}) + 2R_{\delta}(\frac{\tan\delta}{1 + \tan\delta})^2 \\ &+ 16R_{\delta}\{\frac{R_{in} + R_{on} + (R_{in} + R_{on} + R_{\delta}) \tan\delta}{R_{\delta}(1 + \tan\delta)}\}^2. \end{aligned} \tag{14}$$

Here, the dielectric loss tangent $\tan\delta$ is given by

$$\tan\delta = \frac{1}{2\pi f C R_{\delta}}. \tag{15}$$

Hence, Eq.(14) can be rewritten as

$$R_{SC} = 4(R_{in} + R_{on}) + \frac{2R_{\delta}}{(1 + 2\pi f C R_{\delta})^2}$$

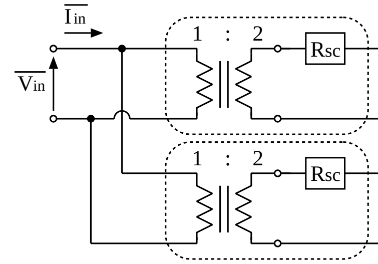

Fig.6 Equivalent circuit of proposed converter.

$$+\frac{16}{R_\delta}\{\frac{2\pi fCR_\delta(R_{in}+R_{on})+(R_{in}+R_{on}+R_\delta)}{1+2\pi fCR_\delta}\}^2. \tag{16}$$

The equivalent circuit of Fig.5 can be expressed by the determinant using Kettenmatrix. Therefore, by using Eqs.(6) and (16), the equivalent circuit of the converter block can be given by the following determinant:

$$\begin{bmatrix} \overline{V_{in}} \\ \overline{I_{in}} \end{bmatrix} = \begin{bmatrix} 1/2 & 0 \\ 0 & 2 \end{bmatrix} \begin{bmatrix} 1 & R_{SC} \\ 0 & 1 \end{bmatrix} \begin{bmatrix} \overline{V_{out}} \\ -\overline{I_{out}} \end{bmatrix}. \tag{17}$$

Hence, from Eq.(17), the equivalent circuit of the proposed converter can be expressed by the circuit shown in Fig.6. From Fig.6, the power efficiency η can be given by

$$\begin{aligned} \eta &= \frac{(\overline{I_{out}})^2R_L}{(\overline{I_{out}}/2)^2R_{SC}+(\overline{I_{out}}/2)^2R_{SC}+(\overline{I_{out}})^2R_L} \\ &= \frac{R_L}{R_{SC}/2+R_L}. \end{aligned} \tag{18}$$

Especially, when the input voltage is a rectangular wave (i.e. $R_\delta=\infty$), the efficiency η can be expressed by

$$\eta=\frac{R_L}{2(R_{in}+R_{on})+R_L}, \tag{19}$$

because the resistance R_{SC} can be expressed from Eq.(14) as

$$R_{SC}=4(R_{in}+R_{on}). \tag{20}$$

The comparison of the power efficiency between the proposed converter and the conventional converter will be discussed in Appendix.

3.2 Ripple Voltage

In this subsection, the ripple voltage of the converter block-1 is analyzed by assuming that $R_{\delta 1}=R_{\delta 2}=\infty$. In $State-T2$, we define that the electric charge $2\Delta Q$ consumed by the output load R_L is charged in C_{1+}. Then, $2\Delta Q$ can be expressed by

$$2\Delta Q=\overline{I_L}(1-D)T, \tag{21}$$

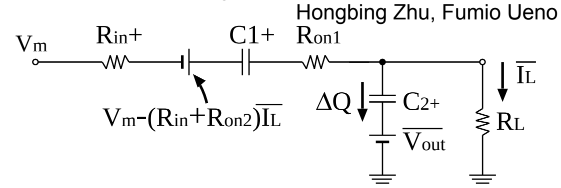

Fig.7 Instantaneous equivalent circuit in $State-T1$.

where $\overline{I_L}$ denotes an averaged charge current of C_{1+}. In the steady state, the instantaneous equivalent circuit of Fig.4 (a) can be rewritten as the circuit shown in Fig.7, where V_m and $\overline{V_{out}}$ denote a positive maximum value of the input voltage and an averaged output voltage, respectively. From Fig.7, by assuming the steady state, the following equation can be obtained by Kirchhoff's voltage law:

$$\begin{aligned} &2V_m-(R_{in}+R_{on2})\overline{I_L} \\ &\quad =\overline{V_{out}}+(R_{in}+R_{on1})(\overline{I_L}+2\Delta Q/DT) \\ &\quad +\Delta Q/C_{2+}+(\Delta Q+\overline{I_L}DT/2)/C_{1+} \end{aligned}$$

and

$$\overline{V_{out}}=\overline{I_L}R_L. \tag{22}$$

From Eqs.(21) and (22), the averaged output voltage $\overline{V_{out}}$ can be given by

$$\overline{V_{out}} = \frac{2DR_LV_m}{Dm}, \tag{23}$$

where

$$\begin{aligned} Dm &= \{(D+1)R_{in}+DR_L+R_{on1}+DR_{on2}\} \\ &\quad +\frac{DT}{2}(\frac{1-D}{C_{2+}}+\frac{1}{C_{1+}}). \end{aligned}$$

When the converter block satisfies the conditions of Eq.(10), Eq.(23) can be rewritten as

$$\overline{V_{out}} = \frac{8CR_LV_m}{4C\{3(R_{in}+R_{on})+R_L\}+3T}. \tag{24}$$

Here, from Fig.7 and Eqs.(21) and (22), the ripple voltage of the converter block-1, V_{rip-1}, can be expressed by

$$\begin{aligned} V_{rip-1} &= \frac{\Delta Q}{C} \\ &= \frac{\overline{I_L}(1-D)T}{2C}=\frac{T}{4CR_L}\cdot\overline{V_{out}}. \end{aligned} \tag{25}$$

Table 1 Size of transistors used in simulations.

Transistor	Size
M_{1+}, M_{1-}	L=1.48 μm, W=17.76 μm
M_{2+}, M_{2-}	L=1.48 μm, W=8.88 μm

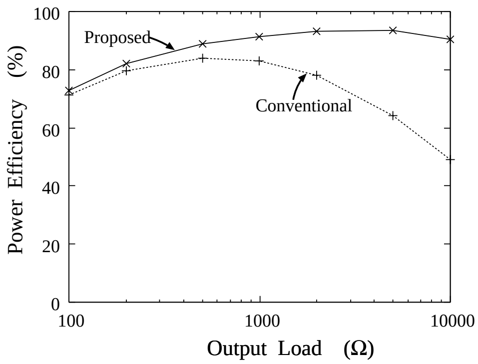

Fig.8 Simulated power efficiency.

4 Simulation

To confirm the effectiveness of the proposed converter, SPICE simulations were performed concerning the circuit shown in Figs.1 and 3. To be compatible with process limitations on the maximum allowable voltage on a chip, we adopted a 2-metal 2-poly 1.2 μm CMOS process. The size of transistors used in SPICE simulations is shown in Table 1.

Figure 8 shows the simulated power efficiency. The SPICE simulations of Fig.8 were performed under the conditions that $V_{in+} = -V_{in-}$ = 1V@40MHz, $C_{1+} = C_{1-} = C_{2+} = C_{2-}$ = 500pF, and R_{in} = 0.1 Ω. As Fig.8 shows, the proposed converter can improve the power efficiency [4] . When the output load is 500 Ω, the power efficiency of the proposed converter is more than 88 % and the electric power is about 5 mW.

Figure 9 shows the simulated ripple voltage. As Fig.9 shows, the ripple voltage of the proposed converter and the conventional converter is almost the same. When the output load is 500 Ω, the ripple voltage is about 0.03 V.

5 Experiment

To confirm the validity of circuit design, the experiment was performed regarding to the proposed circuit shown in Fig.3. The experimental circuit was built with a FCZ1.9-type coil and commercially available transistors 2SK214 and 2SJ77 on a bread board.

[4]The comparison of the power efficiency between the proposed converter and the conventional converter will be discussed in Appendix.

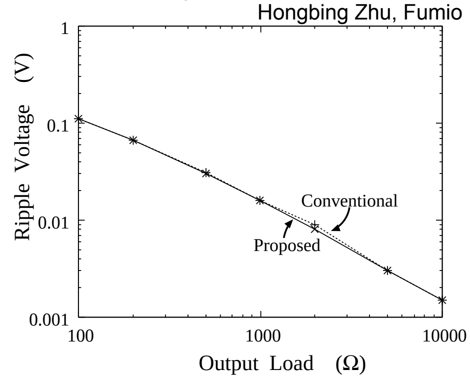

Fig.9 Simulated ripple voltage.

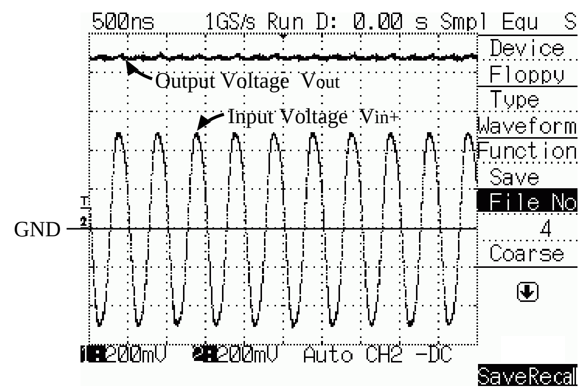

Fig.10 Experimental result.

Figure 10 shows the result of AC-DC conversion obtained by the experimental circuit. In Fig.10, the experiment was performed under the conditions that the AC input voltage V_{p-p} = 1V at 2 MHz and the capacitors $C_{1+} = C_{1-} = C_{2+} = C_{2-}$ = 10nF. As Fig.10 shows, the proposed converter can achieve AC-DC conversion [5] .

6 Conclusion

In this paper, a cross-coupled type AC-DC converter for RFID tags has been proposed. By using cross-coupled connection of CMOS switches, the proposed converter can achieve an AC-DC conversion at high efficiency.

The SPICE simulations showed that 1. the power efficiency of the proposed converter is more than 88

[5]In the experiment, the circuit properties such as power efficiency, ripple noise, etc. were not examined, because the experimental circuit was built with commercially available transistors on the bread board. Only the circuit design was verified through this experiment. The IC implementation and experiments are left to the future study.

%, 2. the electric power is about 5 mW when the output load is 500 Ω, and 3. the ripple voltage and the circuit size of the proposed converter are almost the same as that of the conventional converter. Furthermore, the formulas obtained by the theoretical analyses will be useful for designing the proposed converter.

Due to the limitation of the speed of MOSFET's, the proposed converter will be applied for low and high frequency (134 KHz & 13.56MHz) tags such as package delivery, access control, and payment devices. The IC implementation and experiments are left to the future study.

Acknowledgements: This work is supported by the Ministry of Education, Culture, Sports, Science and Technology, Grant-in-Aid for Scientific Research (B), 18360184, 2007. And the CAD tools used in this work is supported by VLSI Design and Education Center (VDEC), the University of Tokyo in collaboration with On-Semiconductor, Nippon Motorola LTD., HOYA Corporation, and KYOCERA Corporation.

References:

[1] S.Shepard, RFID: Radio Frequency Identification, *New York: McGraw-Hill*, 2005.

[2] K.Rongsawat and A.Thanachayanont, Ultra low power analog front-end for UHF RFID transponder, *Proc. of the International Symposium on Communications and Information Technologies 2006*, 2006, F4D-1 (CD-ROM).

[3] N.Rueangsri and A.Thanachayanont, Coil design for optimum operating range of magnetically-coupled RFID system, *Proc. of the International Symposium on Communications and Information Technologies 2006*, 2006, F4D-2 (CD-ROM).

[4] J.H.Choi, D.Lee, Y.Youn, H.Jeon, and H.Lee, "Scanning-based pre-processing for enhanced RDIF Tag anti-collision protocols," *Proc. of the International Symposium on Communications and Information Technologies 2006*, 2006, F4D-4 (CD-ROM).

[5] T.Tammet, J.Vain, and A.Kuusik, "Using RFID tags for robot swarm cooperation," *WSEAS Transactions on Systems*, Issue 5, Vol.5, 2006, pp.1121-1128.

[6] H.R.Choi, N.K.Park, B.J.Park, D.H.Yoo, H.K.Kwon, and J.J.Shin, "Design of RFID technology-based automated gate system in a container terminal," *WSEAS Trans. on Systems*, Issue 9, Vol.5, 2006, pp.2155-2163.

[7] M.S.Vlad and V.Sgarciu, "A RFID system designed for intelligent manufacturing process," *WSEAS Trans. on Information Science & Applications*, Issue 1, Vol.4, 2007, pp.36-41.

[8] C.C.Tsai, K.F.Kual, and T.Y.Lee, "An RF circuit design of transmission interface for ISO14443A RFID transponders," *WSEAS Trans. on Circuits & Systems*, Issue 8, Vol.6, 2007, pp.532-538.

[9] B.Ju, K.Kim, Y.Yoon, and Y.Lim, "Combined RFID with sensor of motion detect for Security system," *Proc. of the 2007 WSEAS Int. Conference on Circuits, Systems, Signal and Telecommunications*, 2007, pp.221-225.

[10] T.Yamakawa, T.Inoue, S.Hino, E.Ichihara, Y.Takamune, S.Eto, T.Takenaka, J.Chiyonaga, and A. Tsuneda, A circuit design of a smart RF ID tag for heartbeat signal extraction, *47th Mid west Symposium on Circuits and Systems Proceedings*, 2004, pp.III-307 -310.

[11] T.Yamakawa, T.Inoue, S.Eto, T.Takenaka, J.Chiyonaga, and A.Tsuneda, A smart RF ID tag circuit for mouse's heartbeat signal extraction, *2004 IEEJ International Analog VLSI Workshop Proceedings*, 2004, pp.227-232.

[12] T.Yamakawa, T.Inoue, S.Eto, J.Chiyonaga, T.Takenaka, T.Umeda, and A.Tsuneda, An advanced design of a smart RF ID tag circuit for heartbeat signal extraction, *2005 IEEJ International Analog VLSI Workshop Proceedings*, 2005, (CD-ROM).

[13] C.Song, T.Inoue, S.Eto, T.Yamakawa, and A.Tsuneda, Design of an integrated CMOS power supply for wireless power feeding to a smart RFID tag, *2006 IEEJ International Analog VLSI Workshop Proceedings*, 2006, (CD-ROM).

[14] I.Oota, F.Ueno, T.Inoue, and H.B.Lian, Realization and analysis of new switched-capacitor AC-DC converters, *T. IEICE*, Vol.E72, No.12, 1989, pp.1292-1298.

[15] N.Hara, I.Oota, F.Ueno, and I.Harada, A programmable ring type switched-capacitor AC-DC converter, *Proc. of the International Symposium on Nonlinear Theory and its Applications*, Vol.1, 1999, pp.159-162.

[16] S.Terada, I.Oota, K.Eguchi, and F.Ueno, A ring-type switched-capacitor (SC) programmable converter with DC or AC input/DC or AC output, *Proc. of the 47th IEEE International Midwest Symposium on Circuits and Systems*, Vol.I, 2004, pp.29-32.

[17] S.Terada, I.Oota, K.Eguchi, and F.Ueno, A switched-capacitor (SC) AC-DC or AC-AC converter with arbitrarily output voltage using the same circuit configuration, *Proc. of 37th IEEE Power Electronics Specialists Conference*, 2006, pp.1884-1887.

[18] T.Tanzawa and T.Tanaka, A dynamic analysis of the Dickson charge pump circuit, *T.IEEE, Solid-State Circuits*, Vol.32, No.8, 1997, pp.1237-1240.

[19] J.T.Wu and K.L.Chang, MOS charge pumps for low-voltage operation, T.IEEE, Solid-State Circuits, Vol.33, No.4, 1998, pp.592-597.

[20] T.Myono, A.Uemoto, S.Kawai, E.Nishibe, S.Kikuchi, T.Iijima, and H.Kobayashi, High-efficiency charge-pump circuits with large current output for mobile equipment applications, *T.IEICE, Electron.*, Vol.E84-C, No.10, 2001, pp.1602-1611.

[21] H.San, H.Kobayashi, T.Myono, T. Iijima, and N. Kuroiwa, Highly-efficient low-voltage-operation charge pump circuits using bootstrapped gate transfer switches, T.IEEJ, Vol.120-C, No.10, 2000, pp.1339-1345.

[22] K.Eguchi, H.Zhu, T.Tabata, F.Ueno, and T.Inoue, Design of a Dickson-type power converter with bootstrapped gate transfer switches, T. IEEJ, Vol.J124-C, No.7, 2004, pp.1416-1421.

[23] N.Hara, I.Oota, F.Ueno, and T.Inoue, A new ring type set-up switched-capacitor DC-DC converter with low inrush current at start-up and low current ripple in steady state, *T. IEEJ*, Vol.J81-C-II, No.7, 1998, pp.600-612.

[24] N.Hara, I.Oota, I.Harada, and F.Ueno, Programmable ring type switched-capacitor DC-DC converters, *T. IEEJ*, Vol.J82-C-II, No.2, 1999, pp.56-68.

[25] K.Eguchi, F.Ueno, H.Zhu, T.Tabata, and T.Inoue, Design of a charge-average type SC DC-DC converter for cellular phone, *T. IEEJ*, Vol.125-C, No.1, 2005, pp.37-42.

7 Appendix

To save space, only the power efficiency of the conventional converter of Fig.1 is analyzed, because the ripple voltage of the proposed converter and the conventional converter is almost the same as shown in Fig.9.

Firstly, the diode-switch is modeled by the circuit shown in Fig.11. In Fig.11, V_{th} is a voltage source to model the threshold voltage, r_{fk} $(k = 1, 2)$ denotes an on-resistance of the diode-switch, and D_i denotes an $ideal$ diode whose on-resistance is zero. Here, it is known that the diode current can be expressed by

$$I = I_s\{e^{qV/(k_B T_a)} - 1\}, \tag{26}$$

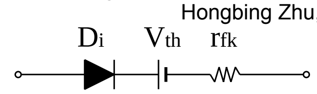

Fig.11 Model of diode-switch.

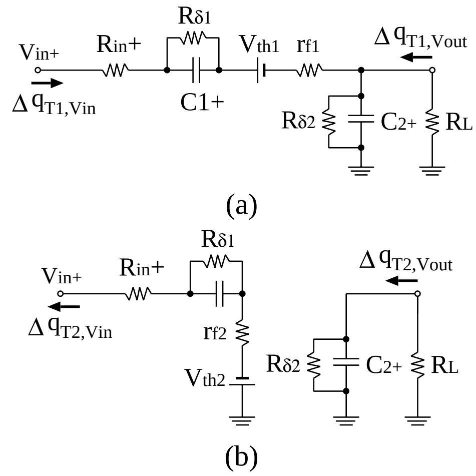

Fig.12 Instantaneous equivalent circuits of the conventional converter block. (a) $State - T1$. (b) $State - T2$.

where I_s, T_a, and k_B denote a saturation current, an absolute temperature, and the Boltzmann's constant, respectively. From Eq.(26), r_{fk} can be derived as follows:

$$\begin{aligned} r_{fk} &= (\frac{dI}{dV})^{-1} = \frac{k_B T_a}{q I_s e^{qV/(k_B T_a)}}, \\ &\simeq \frac{k_B T_a}{qI}. \end{aligned} \tag{27}$$

From Figs.1 and 11, the instantaneous equivalent circuits of the converter block are expressed by the circuits shown in Fig.12.

For easy understanding of the circuit operation, let us consider the converter block-1. In the case of $State - T1$, the differential values of the electric charges in the input and the output terminals, $\Delta q_{T1,V_{in}}$ and $\Delta q_{T1,V_{out}}$, are given by

$$\begin{aligned} & \Delta q_{T1,V_{in}} = \Delta q^1_{T1}(1 + \tan\delta_1) \\ \text{and} \quad & \Delta q_{T1,V_{out}} = \Delta q^2_{T1}(1 + \tan\delta_2) \\ & \qquad - \Delta q^1_{T1}(1 + \tan\delta_1), \end{aligned} \tag{28}$$

respectively. On the other hand, in the case of $State - T2$, $\Delta q_{T2,V_{in}}$ and $\Delta q_{T2,V_{out}}$, are given by

$$\begin{aligned} & \Delta q_{T2,V_{in}} = \Delta q^1_{T2}(1 + \tan\delta_1) \\ \text{and} \quad & \Delta q_{T2,V_{out}} = \Delta q^2_{T2}(1 + \tan\delta_2), \end{aligned} \tag{29}$$

respectively. Since the electric charges in the input and the output, $\Delta q_{V_{in}}$ and $\Delta q_{V_{out}}$, can be expressed by Eq.(5), the following equations are derived by substituting Eqs.(28) and (29) into Eq.(5):

$$\begin{aligned} \Delta q_{V_{in}} &= 2\Delta q_{T1}^1(1+\tan\delta_1), \\ \Delta q_{V_{out}} &= -\Delta q_{T1}^1(1+\tan\delta_1), \\ \text{and} \qquad \overline{I_{in}} &= -2\overline{I_{out}}. \end{aligned} \tag{30}$$

In Fig.12, the energy consumed by resistors in 1-period, W_{SC}, can be expressed by

$$W_{SC} = W_{T1} + W_{T2}, \tag{31}$$

where

$$W_{T1} = \frac{(R_{in}+r_{f1})\cdot\{\Delta q_{T1}^1(1+\tan\delta_1)\}^2}{T1} + \frac{R_{\delta 1}\cdot(\Delta q_{T1}^1\tan\delta_1)^2}{T1} + \frac{R_{\delta 2}\cdot(\Delta q_{T1}^2\tan\delta_2)^2}{T1}$$

and

$$W_{T2} = \frac{(R_{in}+r_{f2})\cdot\{\Delta q_{T2}^1(1+\tan\delta_1)\}^2}{T2} + \frac{R_{\delta 2}\cdot(\Delta q_{T2}^2\tan\delta_2)^2}{T2}.$$

In Fig.12 (a) and (b), the following equations can be obtained by Kirchhoff's law:

$$\begin{aligned} (\overline{V_{in}} - V_{th1})T1 &= R_{\delta_2}\Delta q_{T1}^2\tan\delta_2 \\ &- R_{\delta_1}\Delta q_{T1}^1\tan\delta_1 \\ &- (R_{in}+r_{f1})(1+\tan\delta_1)\Delta q_{T1}^1 \end{aligned}$$

and

$$\begin{aligned} -(\overline{V_{in}} - V_{th2})T2 = R_{\delta_1}\Delta q_{T2}^1\tan\delta_1 \\ + (R_{in}+r_{f2})(1+\tan\delta_1)\Delta q_{T2}^1. \end{aligned} \tag{32}$$

Here, we define that $V_{th} \equiv V_{th1} = V_{th2}$. By substituting Eqs.(2) and (10) into (32), the following equation is obtained:

$$\begin{aligned} \Delta q_{T1}^2\tan\delta = -\frac{2\Delta q_{V_{out}}}{R_\delta(1+\tan\delta)} \\ \cdot\{R_{in}+r_f+(R_{in}+R_\delta+r_f)\tan\delta\}, \end{aligned} \tag{33}$$

where

$$r_f \equiv \frac{r_{f1}+r_{f2}}{2}.$$

Therefore, we can derive the following equations by substituting Eq.(33) into Eq.(31):

$$\begin{aligned} W_{T1} &= 2(R_{in}+r_{f1})\frac{(\Delta q_{V_{out}})^2}{T} \\ &+ 2R_\delta\left(\frac{\tan\delta}{1+\tan\delta}\right)^2\frac{(\Delta q_{V_{out}})^2}{T} \\ &+ 2R_\delta\left[\frac{2\{R_{in}+r_f+(R_{in}+R_\delta+r_f)\tan\delta\}}{R_\delta(1+\tan\delta)}\right]^2 \\ &\cdot\frac{(\Delta q_{V_{out}})^2}{T} \end{aligned}$$

and

$$\begin{aligned} W_{T2} &= 2(R_{in}+r_{f2})\frac{(\Delta q_{V_{out}})^2}{T} \\ &+ 2R_\delta\left[\frac{2\{R_{in}+r_f+(R_{in}+R_\delta+r_f)\tan\delta\}}{R_\delta(1+\tan\delta)}\right]^2 \\ &\cdot\frac{(\Delta q_{V_{out}})^2}{T}. \end{aligned} \tag{34}$$

Since the consumed energy W_{SC} in Fig.6 is defined by Eq.(13), the resistance R_{SC} of the conventional converter block is obtained by Eqs.(13) and (34) as follows:

$$\begin{aligned} R_{SC} = 4(R_{in}+r_f) + 2R_\delta\left(\frac{\tan\delta}{1+\tan\delta}\right)^2 \\ +16R_\delta\left\{\frac{R_{in}+r_f+(R_{in}+R_\delta+r_f)\tan\delta}{R_\delta(1+\tan\delta)}\right\}^2. \end{aligned} \tag{35}$$

Hence, from Eqs.(30) and (35), the equivalent circuit of the proposed converter can also be expressed by the circuit shown in Fig.7. The difference between the proposed converter and the conventional converter is R_{SC}.

From Eqs.(14), (18), and (35), the power efficiency of the conventional converter and the proposed converter is the same if $R_{on} = r_f$. As Eq.(27) shows, however, r_f is in inverse proportion to the diode current I. In other word, r_f becomes large when the output load R_L is large, because I decreases in proportion to R_L. Therefore, in the conventional converter, the power efficiency η decreases greatly at high R_L. This result agrees well with the simulation result of Fig.9.